J|A|C|S
ARTICLES
Published on Web 07/01/2004

# Characterization of Superparamagnetic "Core−Shell" Nanoparticles and Monitoring Their Anisotropic Phase Transition to Ferromagnetic "Solid Solution" Nanoalloys

Jong-Il Park,[†] Min Gyu Kim,[‡] Young-wook Jun,[†] Jae Sung Lee,[‡] Woo-ram Lee,[§] and Jinwoo Cheon*,[§]

*Contribution from the Department of Chemistry, Korea Advanced Institute of Science and Technology, Daejeon 305-701, Korea, Pohang Accelerator Laboratory (PAL) and Department of Chemical Engineering, Pohang University of Science and Technology, Pohang 790-784, Korea, and Department of Chemistry, Yonsei University, Seoul 120-749, Korea*

Received January 20, 2004; E-mail: jcheon@alchemy.yonsei.ac.kr

***Abstract:*** The structure, magnetism, and phase transition of core−shell type CoPt nanoparticles en route to solid solution alloy nanostructures are systematically investigated. The characterization of $Co_{core}Pt_{shell}$ nanoparticles obtained by a "redox transmetalation" process by transmission electron microscopy (TEM) and, in particular, X-ray absorption spectroscopy (XAS) provides clear evidence for the existence of a core−shell type bimetallic interfacial structure. Nanoscale phase transitions of the $Co_{core}Pt_{shell}$ structures toward *c*-axis compressed face-centered tetragonal (fct) solid solution alloy CoPt nanoparticles are monitored at various stages of a thermally induced annealing process and the obtained fct nanoalloys show a large enhancement of their magnetic properties with ferromagnetism. The relationship between the nanostructures and their magnetic properties is in part elucidated through the use of XAS as a critical analytical tool.

## Introduction

The fabrication of advanced nanostructures with exceptional magnetic and optoelectronic properties is a prerequisite for their successful utilization in next generation nanotechnology applications such as tera-level information storage and optical probes for biomedical applications.[1−4] Multicomponent core−shell or solid solution alloy nanostructures are emerging as the most promising solutions for fulfilling these requirements.[2,3,5,6] In particular, multimetallic nanoparticles can exhibit enhanced nanoscale properties and are of particular interest due to their potential as highly efficient catalysts and as independent magnetic components for ultrahigh density memory devices as well as in the biomedical field as magnetic sensors.[1,7−12] Elucidating the phase transition processes that occur as the constituent elements form their novel alloy structures is also a critical step in further enhancing the desired physical properties, as it has been demonstrated for bimetallic catalysts, ferromagnetic nanostructures, and semiconductor quantum dots.[2,6,11]

Although core−shell type heterometallic nanoparticles are of importance, the traditional synthetic approaches have not been successful in producing high quality core−shell nanoparticles. These difficulties are due to several factors including random nucleation processes and inhomogeneous growth of the heterometallic component on top of the seeding host nanomaterials.[13] Similarly, the precise structural characterization and the understanding of the alloying process of core−shell nanoparticles occurring in the nanoscale regime have been very limited, partly due to the lack of well-defined model systems and difficulties in characterization.

Here we choose magnetic nanomaterials of CoPt as a model system in order to understand the alloying process that is so critical in systems which exhibit magnetic properties such as high magnetic anisotropy and magnetooptic Kerr effects.[14] For the nanofabrication of well-defined core−shell type CoPt nanoparticles, a redox transmetalation process has been per-

[†] Korea Advanced Institute of Science and Technology.
[‡] Pohang University of Science and Technology.
[§] Yonsei University.

(1) (a) Klabunde, K. J. *Nanoscale Materials in Chemistry*; Wiley-Interscience: New York, 2001. (b) Pole, C. P.; Owens, F. J. *Introduction to Nanotechnology*; Wiley-Interscience: New Jersey, 2003. (c) Pileni, M. P. *Metal Nanoparticles: Synthesis, Characterization, and Applications*; Marcel Dekker: New York, 2001. (d) Schmid, G. *Clusters and Colloid: From Theory to Application*; Wiley-VCH: Weinheim, 1994.
(2) Sun, S.; Murray, C. B.; Weller, D.; Folks, L.; Moser, A. *Science* **2000**, *287*, 1989.
(3) Klimov, V. I.; Mikhailovsky, A. A.; Xu, S.; Malko, A.; Hollingsworth, J. A.; Leatherdale, C. A.; Eisler, H.-J.; Bawendi, M. G. *Science* **2000**, *290*, 314.
(4) Bruchez, M.; Moronne, M.; Gin, P.; Weiss, S.; Alivisatos, A. P. *Science* **1998**, *281*, 2013.
(5) Zhong, X.; Han, M.; Dong, Z.; White, T. J.; Knoll, W. *J. Am. Chem. Soc.* **2003**, *125*, 8589.
(6) Peng, X.; Schlamp, M. C.; Kadavanich, A. V.; Alivisatos, A. P. *J. Am. Chem. Soc.* **1997**, *119*, 7019.
(7) (a) Himpsel, F. J.; Ortega, J. E.; Mankey, G. J.; Willis, R. F. *Adv. Phys.* **1998**, *47*, 511. (b) Jeon, I. J.; Kang, D. W.; Kim, E. D.; Kim, D. H.; Choe, S. B.; Shin, S. C. *Appl. Surf. Sci.* **2002**, *197*−*198*, 639. (c) Pirausx, L.; George, J. M.; Despres, J. F.; Leroy, C.; Ferain, E.; Legras, R.; Ounadjela, K.; Fert, A. *Appl. Phys. Lett.* **1994**, *65*, 2484.
(8) Black, C. T.; Murray, C. B.; Sandstrom, R. L.; Sun, S. *Science* **2000**, *290*, 1131.
(9) Alivisatos, A. P. *Sci. Am.* **2001**, *285*, 67.
(10) Schneider, J. J. *Adv. Mater.* **2001**, *13*, 529.
(11) Toshima, N.; Yonezawa, T. *New J. Chem.* **1998**, 1179.
(12) Gu, H.; Ho, P.-L.; Tsang, K. W. T.; Wang, L.; Xu, B. *J. Am. Chem. Soc.* **2003**, *125*, 15702.
(13) Schmid, G.; Lehnert, A.; Malm, J.-O.; Bovin, J.-O. *Angew. Chem., Int. Ed. Engl.* **1991**, *30*, 874.


**10.1021/ja049649k CCC: $27.50** 

formed. During this process, the Co nanoparticle, which constitutes the core structure, is oxidized while the shell-forming Pt substituent is reduced due to the favorable redox potential between the two metals. This nanoscale fabrication process developed previously by us is advantageous by well-defined shell layer growth and a straightforward preparation method.[15]

Rigorous structural characterizations of 0-D nanomagnets, in particular, bimetallic core−shell and their phase transformation processes to different structures are important. Although transmission electron microscopy (TEM) has been a powerful tool for characterization of nanomaterials, it is limited in the amount of information with respect to the chemical bonding and structural characterization of complex multicomponent materials such as nanoalloys. In contrast, X-ray absorption spectroscopy (XAS) can provide valuable structural and chemical information (e.g., interatomic distance, coordination number, oxidation state of chemical species) about the nanostructures and supplement the TEM data.[16] While XAS studies on noble metals and their alloys have been well explored,[17] those on magnetic nanoparticles are relatively rare. Here, we demonstrate that XAS is critical to prove the formation of 0-D core−shell CoPt nanostructures and to monitor their ferromagnetic phase transitions to solid solution alloy nanostructures in combination with additional methods such as TEM, XRD, and SQUID.

## Experimental Section

**Synthesis of Co Nanoparticles and $Co_{core}Pt_{shell}$ Nanoparticles.** The synthesis was carried out by slight modification of a reported method.[15] Co nanoparticles were synthesized by the thermal decomposition of dicobalt octacarbonyl ($Co_2(CO)_8$) in a toluene solution of sodium bis-(2-ethylhexyl)sulfosuccinate (NaAOT). $Co_{core}Pt_{shell}$ nanoparticles were synthesized by transmetalation between $Pt(hfac)_2$ (hfac = hexafluoroacetylacetonate) (0.375 mmol) and 6.3 nm ($\sigma = 0.5$ nm) Co nanoparticles (0.75 mmol) in a nonane solution containing 0.09 mL of dodecyl isocyanide ($C_{12}H_{25}NC$) as a stabilizer. After refluxing for 6 h, the colloidal $Co_{core}Pt_{shell}$ nanoparticles (6.4 nm, $\sigma = 0.6$ nm) are separated from the dark red-black solution in waxy powder form after adding ethanol and centrifugation.

**Phase Transitions of $Co_{core}Pt_{shell}$ Nanoparticles into fct CoPt Nanoparticles.** An aliquot amount of toluene solution (~0.01 mM) containing synthesized $Co_{core}Pt_{shell}$ nanoparticles was dropped on the Si(100) wafer (5 mm × 5 mm) and slowly dried for 30 min. Then, $Co_{core}Pt_{shell}$ nanoparticles coated on Si wafer were thermally annealed at the constant temperature (600, 700 °C) of an electrical furnace for 12 h inside a quartz tube under vacuum. The sample was a shiny black colored thin film after annealing and used for further SQUID and XRD analyses.

For the XAS measurement, the powdered $Co_{core}Pt_{shell}$ nanoparticles, annealed under same condition as described above, were mounted in aluminum cells and sealed with polyimide tape (KAPTON-500H, 125 $\mu$m thickness). Samples were formed with a thickness ($d$) of 100 $\mu$m complying the condition that $\Delta\mu x \leq 0.1$, where $x$ is the effective sample thickness ($d/\cos 45°$) and $\Delta\mu$ is the absorbance at both the Co K-edge and Pt $L_{III}$-edge. Sample preparations were carried out in an inert glovebox to prevent any oxidation or contaminations.

**XAS Measurement.** Co K-edge and Pt $L_{III}$-edge X-ray absorption spectra (XAS) were recorded on the BL3C1 beam line of Pohang light source (PLS) with a ring current of 120−170 mA at 2.5 GeV. An Si-(111) double crystal monochromator was used with detuning to 85% in intensity to eliminate the high-order harmonics. The data were collected in transmission mode with the nitrogen (85%) and argon (15%) gas-filled ionization chambers as detectors. Energy calibrations were carried out with the Co and Pt metal foils, assigning the first inflection point to 7709 and 11564 eV, respectively. To remove an energy shift problem, X-ray absorption spectra for Co and Pt metal foils were measured simultaneously in every measurement as the metal foils were positioned before the window of the third ion chamber.

**Co K-Edge and Pt $L_{III}$-edge EXAFS Data Analysis.** The EXAFS data analyses were carried out by the standard procedure. The measured absorption spectra below the preedge region were fitted to a straight line, and then the background contributions above the postedge region, $\mu_o(E)$, were fitted to a fourth order polynomial (cubic spline). The fitted polynomials were extrapolated through the total energy region and subtracted from the total absorption spectra. The background-subtracted absorption spectra were normalized for the above energy region, $\chi(E) = \{\mu(E)\mu_o(E)\}/\mu_o(E)$. The normalized $k^3$- and $k^2$-weighted EXAFS spectra, $k^3\chi(k)$ and $k^2\chi(k)$, were Fourier transformed in the $k$ range from 2.0 to 14.5 Å$^{-1}$ to show the contribution of each bond pair on the Fourier transform (FT) peak. The experimental Fourier-filtered spectra could be obtained from the inverse Fourier transformation with the hanning window function in the $r$ space range between 1.0 and 6.0 Å. To determine the structural parameters for each bond pair, the curve fitting process was carried out by using the EXAFS formula, which is expressed as follows:

$$\chi(k) = \sum N_j S_i^2(k) F_j(k) \exp(-2\sigma_j^2 k^2) \times \left(\exp(-2r_j/\lambda_j(k)) \frac{\sin(2kr_j + \Phi_{ij}(k))}{kr_j^2}\right)$$

which includes the photoelectron wave vector, $k$ (= $[8\pi^2 m(E - E_o)/h^2]^{1/2}$), the coordination number, $N_j$, the amplitude reduction factor, $S_i^2$, the effective curved wave backscattering amplitude, $F_j(k)$, the Debye−Waller factor, $\sigma_j^2$, the mean free path of the photoelectron, $\lambda$, the interatomic distance, $r_j$, and total phase shift, $\Phi_{ij}$, respectively.

Theoretical scattering paths could be obtained from the crystallographic description of the known model. The theoretical EXAFS parameters such as phase shift, backscattering amplitude, and total central atom loss factor were calculated for a function of wavenumber for all possible scattering paths by FEFF6.01 code. For simplicity in curve fitting process, the $S_i^2$ value was fixed to 0.85 for the Co and Pt

(14) (a) Ely, T. O.; Pan, C.; Amiens, C.; Chaudret, B.; Dassenoy, F.; Lecante, P.; Casanove, M.-J.; Mosset, A.; Respaud, M.; Broto, J.-M. *J. Phys. Chem. B* **2000**, *104*, 695. (b) Shevchenko, E. V.; Talapin, D. V.; Rogach, A. L.; Kornowski, A.; Haase, M.; Weller, H. *J. Am. Chem. Soc.* **2002**, *124*, 11480. (c) Sanchez, J. M.; Moran-Lopez, J. L.; Leroux, C.; Cadeville, M. C. *J. Phys.: Condens. Matter* **1989**, *1*, 491. (d) Harp, G. R.; Weller, D.; Rabedeau, T. A.; Farrow, R. F. C.; Toney, M. F. *Phys. Rev. Lett.* **1993**, *71*, 2493.

(15) Preliminary synthetic results of this process have been reported. The reaction byproducts, for example $Co(hfac)_2$, have been isolated and confirmed by various analytical methods. See: Park J.-I.; Cheon, J. *J. Am. Chem. Soc.* **2001**, *123*, 5743.

(16) Rehr, J. J.; Albers, R. C. *Rev. Mod. Phys.* **2000**, *72*, 621.

(17) Previously, XAS has been used to investigate the structural characterization of noble metals and their alloys. (a) Benfield, R. E.; Grandjean, D.; Kröll, M.; Pugin, R.; Sawitowsli, T.; Schmid, G. *J. Phys. Chem. B* **2001**, *105*, 1961. (b) Bradley, J. S.; Via, G. H.; Bonneviot, L.; Hill, E. W. *Chem. Mater.* **1996**, *8*, 1895 (Pd−Cu). (c) Harada, M.; Asakura, K.; Ueki, Y.; Thosima, N. *J. Phys. Chem.* **1993**, *97*, 10742 (Pd−Rh). (d) Molenbroek, A. M.; Haukka, S.; Clausen, B. S. *J. Phys. Chem. B* **1998**, *102*, 10680 (Cu−Pd). (e) Nashner, M. S.; Frenkel, A. I.; Adler, D. L.; Shapley, J. R.; Nuzzo, R. G. *J. Am. Chem. Soc.* **1997**, *119*, 7760 (Pt−Ru). (f) O'Grady, W. E.; Hagans, P. L.; Pandya, K. I.; Maricle, D. L. *Langmuir* **2001**, *17*, 3047 (Pt−Ru). (g) Hills, C. W.; Nashner, M. S.; Frenkel, A. I.; Shapley, J. R.; Nuzzo, R. G. *Langmuir* **1999**, *15*, 690 (Pt−Ru). (h) Nashner, M. S.; Frenkel, A. I.; Somerville, D.; Hills, C. W.; Shapley, J. R.; Nuzzo, R. G. *J. Am. Chem. Soc.* **1998**, *120*, 8093 (core−shell Pt−Ru). (i) Kolb, U.; Quaiser, S. A.; Winter, M.; Reetz, M. T. *Chem. Mater.* **1996**, *8*, 1889 (Pd−Pt). (j) Harada, M.; Asakura, K.; Ueki, Y.; Toshima, N. *J. Phys. Chem.* **1992**, *96*, 9730 (Pd−Pt). (k) Toshima, N.; Harada, M.; Yonezawa, T.; Kushihashi, K.; Asakura, K. *J. Phys. Chem.* **1991**, *95*, 7448 (Pd−Pt). (l) Nashner, M. S.; Somerville, D. M.; Lane, P. D.; Adler, D. L.; Shapley, J. R.; Nuzzo, R. G. *J. Am. Chem. Soc.* **1996**, *118*, 12964 (Re−Ir). (m) Toshima, N.; Harada, M.; Yamazaki, Y.; Asakura, K. *J. Phys. Chem.* **1992**, *96*, 9927 (Au−Pd). (n) Molenbroek, A. M.; Norskov, J. K.; Clausen, B. S. *J. Phys. Chem. B* **2001**, *105*, 5450 (Ni−Au). (o) Shibata, T.; Bunker, B. A.; Zhang, Z.; Meisel, D.; Varderman, C. F.; Gezelter, J. D. *J. Am. Chem. Soc.* **2002**, *124*, 11989 (Au−Ag).

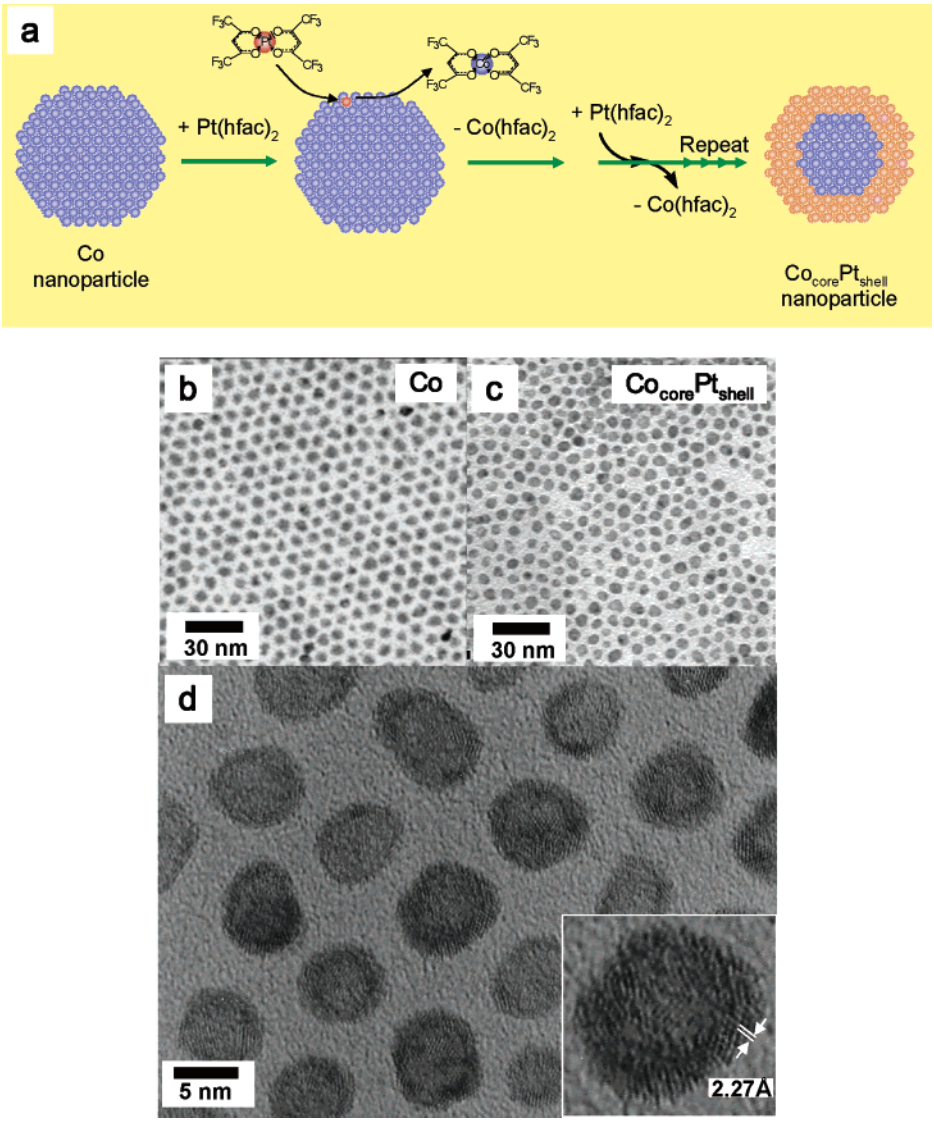


***Figure 1.*** Redox transmetalation process and TEM analysis of $Co_{core}Pt_{shell}$ nanoparticles. (a) Redox transmetalation processes for core−shell nanoparticles. During the reaction, $Pt^{2+}$ of $Pt(hfac)_2$ is reduced to Pt while the surface Co atom of the Co nanoparticles is oxidized via hfac ligand migration to form $Co(hfac)_2$ as a reaction byproduct. Repeating cycles of this reaction results in core−shell bimetallic nanoparticles. TEM images of (b) 6.3 nm Co nanoparticles, (c) $Co_{core}Pt_{shell}$ nanoparticles, and (d) HRTEM images of 6.4 nm $Co_{core}Pt_{shell}$ nanoparticles.

atoms. The coordination number ($N$) was evaluated by independent iteration from the Debye−Waller factor although the $N$ value was correlated with the Debye−Waller factor in the amplitude of EXAFS spectra. The experimental $k^n\chi(k)$ spectra were fitted with possible scattering paths showing the substantial amplitude for the corresponding FT peak. In this case, structural parameters such as the coordination number, the interatomic distance and the Debye−Waller factor were used as adjustable parameters in the fitting process for the EXAFS spectra.

**TEM, XRD, and Magnetic Measurements.** TEM and HRTEM analyses were carried out on an EM 912 Omega, Hitachi H9000-NAR, and JEOL ARM-1300S instruments operated at 120, 300, or 1250 kV, respectively. X-ray diffraction (XRD) spectra were obtained using graphite-monochromatized Cu Kα radiation in a Rigaku D/MAX-RC diffractometer operated at 40 kV 80 mA. Magnetic measurements were performed on a SQUID magnetometer (Quantum Design MPMS-7). The temperature was varied between 5 and 300 K according to a zero-field cooling/field cooling (ZFC/FC) procedure at 75 Oe, and the hysteretic loops were obtained in a magnetic field varying from +5 to −5 T.

## Results and Discussion

**Synthesis and TEM Analysis of $Co_{core}Pt_{shell}$ Nanoparticles.** By utilizing a redox transmetalation process, the synthesis of $Co_{core}Pt_{shell}$ nanoparticles was performed by refluxing 6.3 nm ($\sigma$ = 0.5 nm) Co nanoparticles with $Pt(hfac)_2$, (hfac = hexafluoroacetylacetonate), in a nonane solution containing dodecyl isocyanide as a capping molecule (Figure 1). During the reaction, the $Pt^{2+}$ of $Pt(hfac)_2$ is reduced to Pt while the surface Co atom of the Co nanoparticles is oxidized via hfac ligand migration to form $Co(hfac)_2$ as a reaction byproduct (Figure 1a). Transmission electron microscopy (TEM) images of the obtained CoPt nanoparticles show nanoparticles with an average diameter of 6.4 nm ($\sigma$ = 0.6 nm) (Figure 1c). HRTEM images show relatively well-developed lattice fringe patterns especially in the edge area of the dots (Figure 1d). A measured mean lattice distance of 2.27 Å is consistent with the known Pt lattice parameter (2.265 Å) for the (111) plane. The slightly darker image contrast of the edge area also suggests the

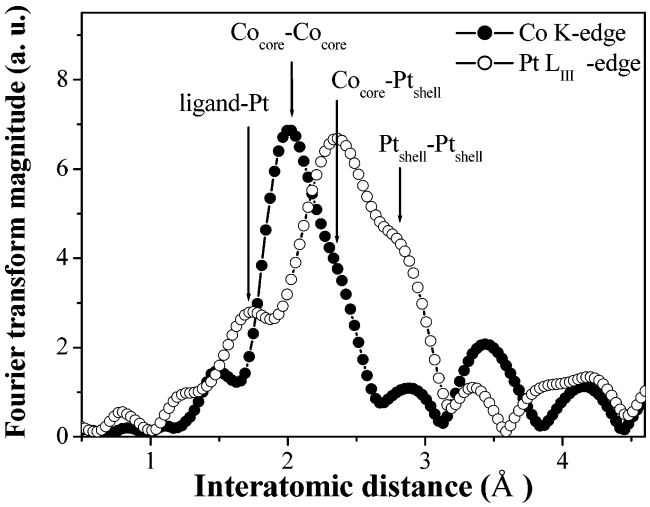


***Figure 2.*** XAS analysis of $Co_{core}Pt_{shell}$ and annealed $Co_{core}Pt_{shell}$ nanoparticles. Fourier transforms of Co K-edge $k^3\chi(k)$ (filled circle) and Pt $L_{III}$-edge $k^2\chi(k)$ EXAFS spectra (open circle) of the $Co_{core}Pt_{shell}$ nanoparticles.

formation of the $Pt_{shell}$ layer and EDS analysis of the nanoparticles indicates the stoichiometry to be $Co_{0.45}Pt_{0.55}$.[18] However, these analyses do not unambiguously prove that the core−shell structures were formed since interferences such as Moiré fringe patterns are also possible.

**XAS Analysis of $Co_{core}Pt_{shell}$ Nanoparticles.** To achieve a better evidence of this core−shell nanostructure formation, X-ray absorption spectroscopic analysis (XAS) was performed.

A strong peak at ∼2.0 Å and a shoulder at ∼2.3 Å (Figure 2, filled circle) appearing in the Fourier transform (FT) of Co K-edge $k^3\chi(k)$ extended X-ray absorption fine structure (EXAFS) spectrum of the CoPt nanoparticles indicates that the first shell around the Co atom includes two different types of neighboring atoms. The peak at ∼2.0 Å is assigned to single scattering by $Co_{core}-Co_{core}$ atoms within the $Co_{core}$ region and the shoulder at ∼2.3 Å corresponds to single scattering by the $Co_{core}-Pt_{shell}$ at core−shell interfaces.

The FT of the Pt $L_{III}$-edge $k^2\chi(k)$ EXAFS spectrum (Figure 2, open circle) suggests three different environments are present for Pt atoms. A strong peak at ∼2.3 Å arising from single scattering of $Co_{core}-Pt_{shell}$ atoms in the interface region is consistently observed while the shoulder at ∼2.7 Å is due to the $Pt_{shell}-Pt_{shell}$ interaction within the Pt shell layer. An additional peak at ∼1.7 Å corresponds to the scattering with capping molecules on the surface of the Pt shell layer. Structural parameters (e.g., interatomic distance, coordination number, and Debye−Waller factor) for the $Co_{core}Pt_{shell}$ structures are obtained from EXAFS refinement (Table 1). These results suggest that the interatomic distance between the $Co_{core}$ and the nearest neighboring Co atom is 2.48 Å which is consistent with the value for the bulk face-centered cubic (fcc) phase of cobalt (2.50 Å). The interatomic distance between Co atom and the neighboring Pt atom is determined to be 2.64 Å which is also in good agreement with the reported value of $Co_1Pt_1$ (2.65 Å). The EXAFS data clearly confirm that the CoPt nanoparticles obtained by this transmetalation reaction are indeed of a core−shell structure of Co and Pt.

(18) TEM image contrasts depend on the mass-thickness of the samples with heavier elements appearing darker than lighter elements and the EDS analysis indicates a moderate degree of Pt incorporation with an estimated thickness of $Co_{core}$ and $Pt_{shell}$ to be roughly 4.6 and 1.8 nm, respectively.

***Table 1.*** Co K-Edge EXAFS Structure Parameters of Co, $Co_{core}Pt_{shell}$, and Annealed $Co_{core}Pt_{shell}$ Nanoparticles (NPs)

| compound | path | $\Delta E$, eV | $N$ | $R$ (Å)[a] | $\sigma^2$ ($\times10^{-3}$ Å$^2$)[a] |
|---|---|---|---|---|---|
| 7 nm Co NPs | Co −Co | −4.3 | 7.1 | 2.49(3) | 8.92 |
| 4 nm Co NPs | Co −Co | −4.3 | 5.2 | 2.49(4) | 8.67 |
| $Co_{core}Pt_{shell}$ NPs | Co −Co | −5.1 | 4.5 | 2.48(2) | 12.5 |
| | Co −Pt | 2.7 | 2.6 | 2.64(1) | 16.1 |
| annealed $Co_{core}Pt_{shell}$ NPs | $A_1$ | −3.1 | 6.1 [8][b] | 2.65(4) | 8.26 |
| | $A_2$ | 5.2 | 1.5 [4] | 2.70(2) | 2.23 |
| | $B_1$ | −0.4 | 1.2 [2] | 3.77(4) | 2.69 |
| | $B_2$ | 9.1 | 2.4 [4] | 4.01(7) | 11.3 |
| | $C_1$ | −8.7 | 4.6 [8] | 4.48(8) | 13.5 |
| | $C_2$ | −9.4 | 9.6 [16] | 4.64(4) | 5.89 |
| | $D_1$ | −5.5 | 3.5 [8] | 5.26(7) | 12.1 |
| | $D_2$ | 5.7 | 2.6 [8] | 5.27(4) | 3.83 |

[a] In curve fitting process, the goodness of fit by $\{\Sigma(k^3\chi_{data} - k^3\chi_{model})^2\}/\Sigma(k^3\chi_{data})^2$ was estimated within allowed error range. The estimated errors are within ±0.02 Å for the interatomic distance and about 15% for the Debye−Waller factor. [b] The expected coordination number of bulk fct CoPt model.

**XAS Analysis upon Phase Transformation of $Co_{core}Pt_{shell}$ into fct CoPt Alloy Nanoparticles.** Tremendous variations in the physical properties of nanomaterials can result from their structural phase transitions. By thermally annealing our initially synthesized core−shell structure under vacuum at 600 or 700 °C for 12 h, its phase transition to solid solution alloy was induced that is crucial for a significant enhancement of its magnetic properties.

Analysis of the FTs of Co K-edge $k^3\chi(k)$ EXAFS spectra indicates that the $Co_{core}Pt_{shell}$ undergoes a transition to structurally different species during the thermal annealing process. Peaks corresponding to Co−Co (fcc) at ∼2.0 Å and Co−Pt at ∼2.3 Å of the core−shell structure appear to shift to peak positions corresponding to greater interatomic distances with an increase in the overall peak intensity (Figure 3a. from bottom to top spectra).[19] A relatively strong and broad first peak from the 600 °C sample contains three deconvoluted peaks, at 2.0, 2.3, and 2.6 Å, corresponding to Co−Co (fcc) and Co−Pt and Co−Co (fct), respectively (Figure 3b middle spectra). The decrease in intensity of the peak at 2.0 Å and the appearance of a peak at 2.6 Å suggest that the fcc packing of the Co core structure now changes into a different Co−Co interaction due to a *c*-axis compressed face-centered tetragonal (fct) structure (vide infra). Finally for the 700 °C sample, the strong first peak possesses two deconvoluted peaks occurring at 2.3 and 2.6 Å, corresponding to Co−Pt and fct Co−Co, respectively (Figure 3a and Figure 3b top spectra). By standard EXAFS fitting process, the structural parameters of Co−Pt and Co−Co for the first shell are obtained as 2.65 and 2.70 Å, which are consistent with 2.65 and 2.69 Å of the fct model. Also, other scattering modes of EXAFS data are well matched with fct $Co_1Pt_1$ model structure. Peak A (∼2.3 and ∼2.6 Å) in Figure 3a is assigned to two scatterings of Co−Pt and Co−Co for the out-of-plane and in-plane direction, respectively (Figure 3c, red arrows $A_1$, $A_2$). The observation of two weaker peaks B (∼3.4 and ∼3.6 Å) suggests single scattering with a Co atom at the (0, 0, 1) and (1, 0, 0) sites from the central Co atom (Figure 3c, blue arrows $B_1$, $B_2$) and double peaks C (∼4.2 Å) correspond to single scatterings

(19) The higher FT magnitude observed after annealing can be due to an increase in the static ordering of Co and Pt site redistribution. Even after annealing at 700 °C, annealed CoPt nanoparticles do not exhibit the formation of a bulk CoPt alloy, which is confirmed by TEM analysis and the FT amplitude of annealed CoPt nanoparticles.

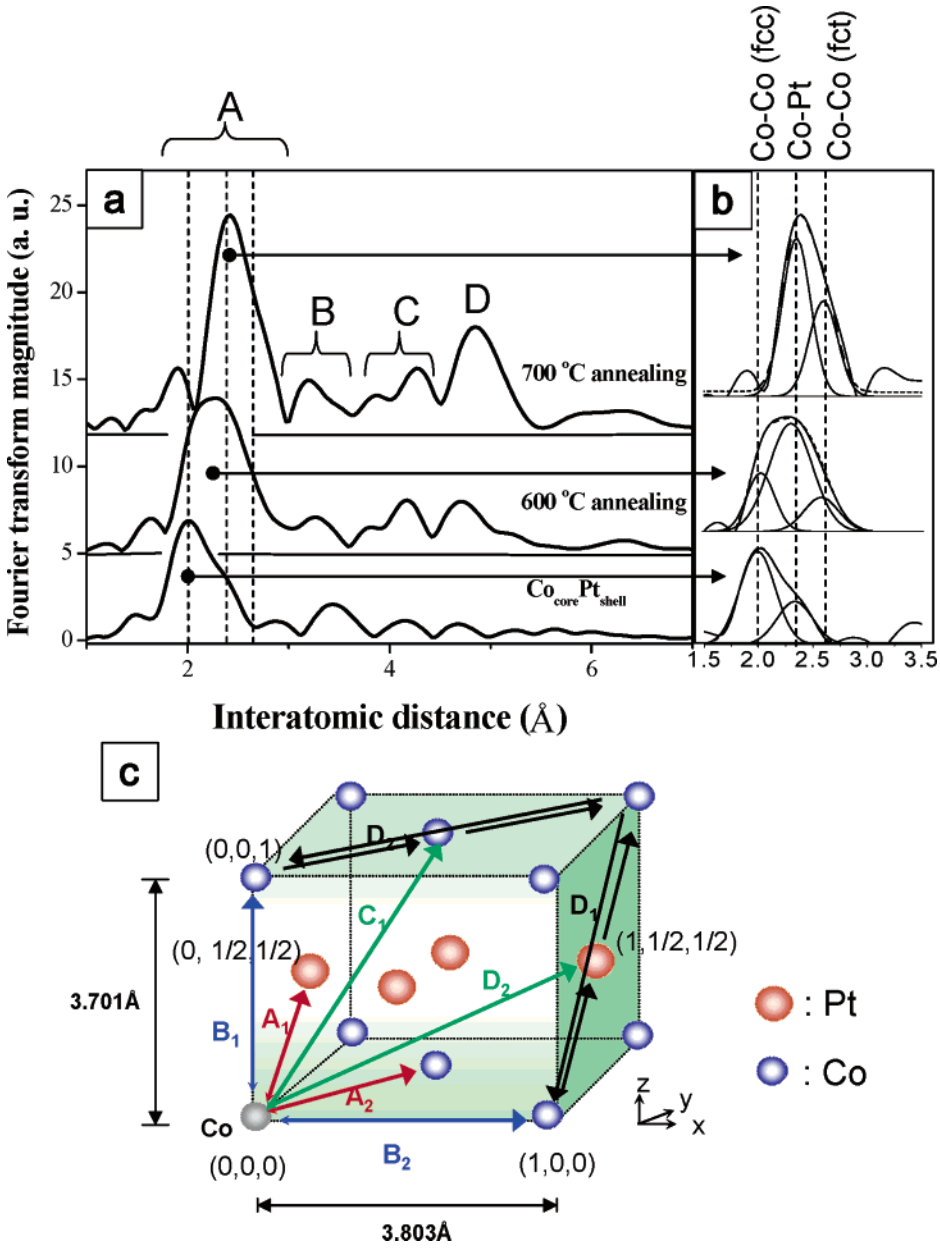


***Figure 3.*** (a) Fourier transforms of Co K-edge $k^3\chi(k)$ EXAFS spectra for $Co_{core}Pt_{shell}$ nanoparticles annealed at 600 °C and 700 °C for 12 h and (b) their peak deconvolutions. The intensity of the first shell Co−Co (fcc) (∼2.0 Å) scattering peak of $Co_{core}Pt_{shell}$ gradually decreases and finally fades out as the annealing temperature increases while the intensities of the first shell Co−Pt (∼2.3 Å) and Co−Co (fct) (∼2.6 Å) scattering peaks increase, indicating phase transformation from $Co_{core}Pt_{shell}$ to fct CoPt solid solution alloys. (c) Face-centered tetragonal crystal model of $Co_1Pt_1$ and scattering modes ($A_{1,2}$, $B_{1,2}$, $C_{1,2}$, $D_{1,2}$) corresponding to the EXAFS spectra of 700 °C sample.

of Pt at the (1, 1/2, 1/2) site and Co at the (1/2, 1/2, 1) site (Figure 3c, green arrows $C_1$, $C_2$). Peak D (∼5.0 Å) results from the overlap of two multiple scatterings for out-of-plane and in-plane, namely, Co(1, 0, 0) → Pt(1, 1/2, 1/2) → Co(1, 1, 1) → Pt(1, 1/2, 1/2) triple scattering and Co(0, 0, 1) → Co(1/2, 1/2, 1) → Co(1, 1, 1) double scatterings, respectively (Figure 3c, black arrows $D_1$, $D_2$). Scattering modes of this peak A and of the smaller peaks labeled B, C, and D at higher atomic distances (Figure 3a top spectrum) are well matched with a model structure of fct $Co_1Pt_1$ alloy (JCPDS 43-1358) whose lattice parameters are $a = 3.803$ Å and $c = 3.701$ Å under the space group of *P*4/*mmm* of tetragonal symmetry (Figure 3c).

Figure 4 shows normalized X-ray absorption near edge structure (XANES) spectra of CoPt nanoparticles. In the Pt $L_{III}$-edge XANES spectra (Figure 4 inset), the successive decrease in white line peak intensity, caused by increased charge transfer from Co to Pt, is indicative of the progression of Co−Pt alloying due to the annealing process. In the Co K-edge XANES spectra (Figure 4), broad white line peaks of $Co_{core}Pt_{shell}$ nanoparticles are separated into distinct peaks labeled B and C after the annealing process, which is a characteristic feature of alloyed CoPt.[20]

Thermally induced dynamic phase transitions of $Co_{core}Pt_{shell}$ nanoparticles [Co−Co(fcc) and Co−Pt] to a solid solution alloy of anisotropically ordered fct CoPt nanoparticles [Co−Pt and

(20) Hill, E. K.; Baudoing-Sanois, R.; Moraweck, B.; Renouprez, A. J. *J. Phys. Chem.* **1996**, *100*, 3102.

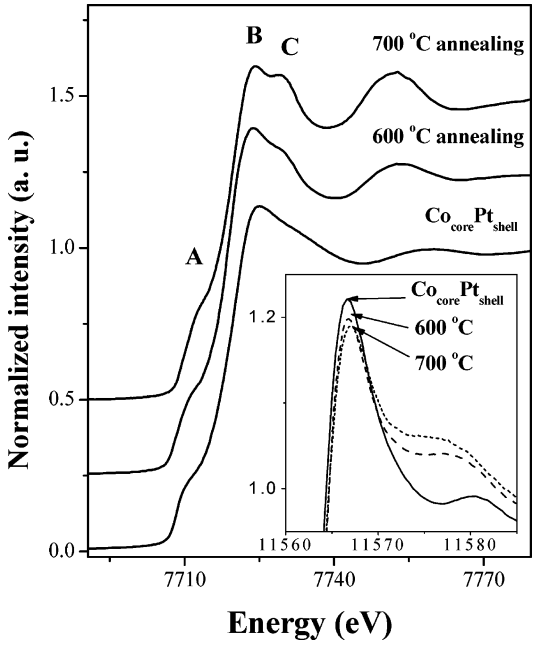


***Figure 4.*** Changes of normalized Co K-edge XANES and Pt $L_{III}$-edge XANES (inset) spectra upon thermal annealing of $Co_{core}Pt_{shell}$ nanoparticles for 12 h. Appearance of distinct peaks of B, C and the successive decrease of peak intensity (inset) indicates the progression of the Co−Pt solid solution alloy formation.

Co−Co(fct)] through a $Co_{core}(CoPt)_{ordered-alloy}Pt_{shell}$ intermediate state via inter-diffusion processes proceed.[21] These XAS results are also consistent with the fct structure obtained from X-ray diffraction studies (Figure 5a).

**Enhanced Magnetism of Phase Transformed CoPt Alloy Nanoparticles.** The effect of the structural phase transition on the magnetic properties is critical. Although $Co_{core}Pt_{shell}$ nanoparticles show superparamagnetism with zero magnetic coercivity ($H_c$) at room temperature (Figure 5c), the $H_c$ at 5 K was remarkably enhanced from 330, to 1300, and finally to 7000 Oe after annealing the $Co_{core}Pt_{shell}$ nanoparticles at 600 and 700 °C for 12 h. The sample annealed at 700 °C shows ferromagnetism with a $H_c$ of 5300 Oe at room temperature (Figure 5d). Our annealed CoPt nanoparticles retain their size (∼ 6 nm) without forming bulk CoPt[22] and are observed to be nanoscale ferromagnets that could potentially be used as magnetic bits for teralevel information storage applications.[23]

The large enhancement of the magnetic properties is closely related to the alloy formation and consistent with the XAS results. Most nanoparticles below the critical size typically show superparamagnetic behavior at room temperature due to a higher thermal fluctuation energy (kT) than anisotropic energy ($K_uV$).[7a] In contrast, the enhanced ferromagnetism of our sample is originated from the increased magnetocrystalline anisotropy (anisotropy constant ($K$) of bulk fct CoPt is $4 \times 10^7$ erg/cm$^3$) of the fct structure which possesses a shorter Co−Pt bond distance in the *c*-axis and an increased number of neighboring

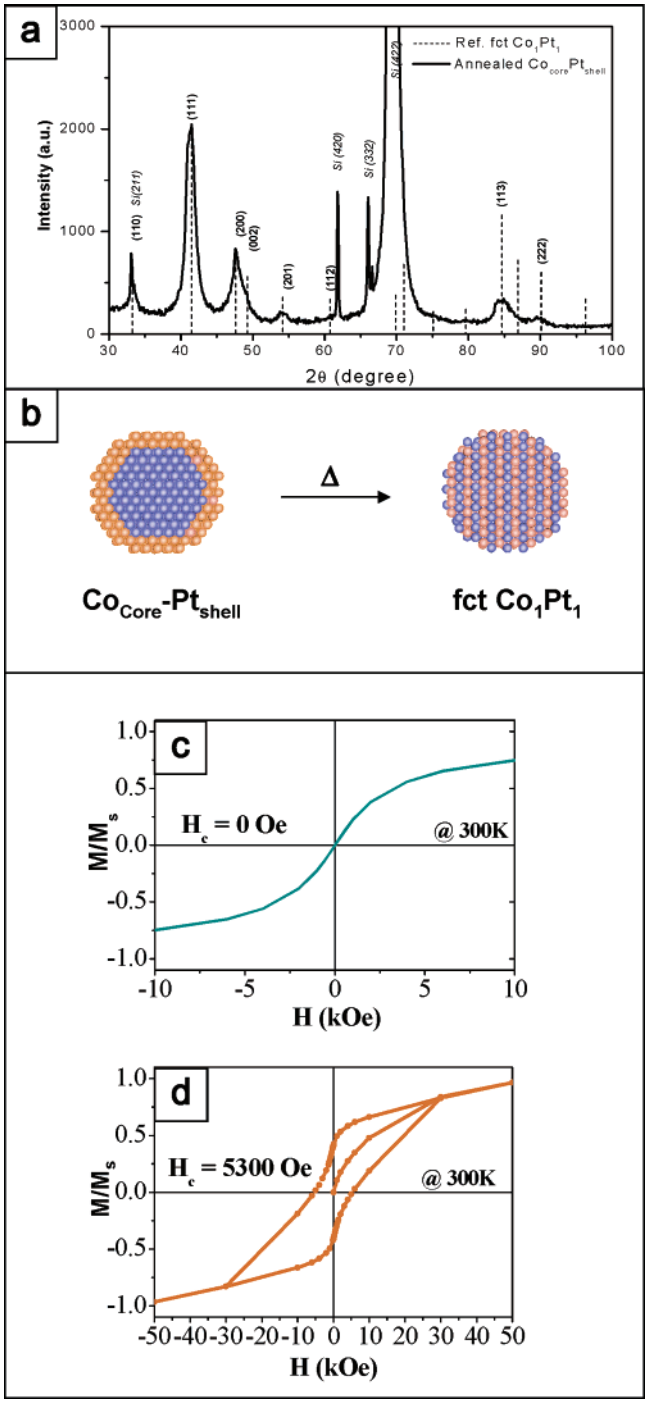


***Figure 5.*** XRD analysis and magnetic properties of $Co_{core}Pt_{shell}$ nanoparticles. (a) XRD pattern of $Co_{core}Pt_{shell}$ nanoparticles annealed at 700 °C for 12 h. All peaks are well matched to reference fct $Co_1Pt_1$ alloys (dashed line). (b) Thermal alloying of $Co_{core}Pt_{shell}$ nanoparticles to anisotropic fct structure. Hysteresis loops of $Co_{core}Pt_{shell}$ nanoparticles measured at 300 K (c) before and (d) after the annealing process at 700 °C. The magnetic coercivity of the nanoparticles is significantly enhanced from 0 to 5300 Oe exhibiting room-temperature ferromagnetism.

Co atoms on the Pt atom when compared with fcc packing modes of core−shell structures (Figure 3c). These anisotropic structural changes induce strong ferromagnetic coupling on Pt and Co atoms due to the hybridization of Pt 5d and Co 3d states and spin polarization of Pt atoms.[14a,24]

(21) Similar formation of ordered inter-diffused CoPt alloy layers in Co/Pt layered structures at high temperatures (500−700 °C) have previously reported, which is consistent with our observations. See: (a) Train, C.; Beauvillain, P.; Mathet, V.; Penissard, G.; Veillet, P. *J. App. Phys.* **1999**, *86*, 3165. (b) Moon, D. W.; et al. *App. Phys. Lett.* **2001**, *79*, 503.

(22) Our EXAFS results are quite consistent with the TEM analysis of annealed CoPt where most CoPt retained their sizes except a very small portion (< ∼8%) of sintered particles (Figure S4 in Supporting Information).

(23) Weller, D.; Moser, A. *IEEE Trans. Magn.* **1999**, *35*, 4423.

(24) Koote, A.; Haas, C.; Groot, R. A. *J. Phys.: Condens. Matter* **1991**, *3*, 1133.

## Conclusion

Nanoscale characterization and correlation of nanostructures to their magnetic properties during the anisotropic phase transitions were successfully examined. The core−shell structure is clearly confirmed and subsequent thermally induced dynamic phase transitions of fcc $Co_{core}Pt_{shell}$ nanoparticles to a solid solution alloy of anisotropically ordered fct CoPt nanoparticles are monitored. Our obtained CoPt alloy nanostructures show a large enhancement of their magnetic properties by exhibiting ferromagnetism at room temperature and overcoming the superparamagnetic limitations of common magnetic nanomaterials. The redox transmetalation process is effective for the formation of core−shell nanostructures, and further synthetic and characterization approaches of this kind may facilitate the development of a wide range of advanced core−shell or alloy nanomaterials and help to attain a better understanding of the intricate relationship between their structure and functionality.

**Acknowledgment.** This work was supported by the National R&D Project for Nano Science and Technology, Korea Science and Engineering Foundation (Grant 1999-1-122-001-5) and the U.S. Department of the Navy (Grant N62649-03-1-0008). We thank KBSI for the TEM and magnetic measurements of samples. We are also grateful to authorities of Pohang Light Source (PLS) for X-ray absorption spectroscopic measurements.

**Supporting Information Available:** Figures of Co K-edge $k^3$-weighted EXAFS spectra of $Co_{core}Pt_{shell}$ nanoparticles and the annealed samples at 600 °C and 700 °C for 12 h (S1), (S2) Co K-edge $k^3$-weighted experimental and best-fitted EXAFS spectra of $Co_{core}Pt_{shell}$ nanoparticles and their Fourier transforms (S1), Co K-edge $k^3$-weighted experimental and best-fitted EXAFS spectra of annealed $Co_{core}Pt_{shell}$ nanoparticles at 700 °C and their Fourier transforms (S3), and a representative TEM image of annealed $Co_{core}Pt_{shell}$ nanoparticles at 700 °C (S4). This material is available free of charge via the Internet at http://pubs.acs.org.

JA049649K